

1 Taxa-driven functional shifts associated with stormflow in an urban stream microbial community

2

3 Adit Chaudhary,<sup>a</sup> Imrose Kauser,<sup>a</sup> Anirban Ray,<sup>a,b</sup> Rachel Poretsky<sup>a#</sup>

4

5 <sup>a</sup>Department of Biological Sciences, University of Illinois at Chicago, Chicago, Illinois, USA

6

7 Running Title: Stormflow impacts on urban stream microbiome

8

9

10 #Author for correspondence

11 Mailing address: University of Illinois at Chicago, Department of Biological Sciences, 950 S.

12 Halsted St., Chicago, IL 60607. Phone: 312-355-5102. Email: [microbe@uic.edu](mailto:microbe@uic.edu).

13

14 Word count for abstract: 239

15 Word count for text: 4394

16

17

18

19

20

21

---

<sup>b</sup> Present address: BioScience Research Collaborative, Rice University, Houston, Texas, USA

## 22 **Abstract**

23 Urban streams are susceptible to stormwater and sewage inputs that can impact their ecological  
24 health and water quality. Microbial communities in streams play important functional roles and  
25 their composition and metabolic potential can help assess ecological state and water quality.  
26 Although these environments are highly heterogenous, little is known about the influence of  
27 isolated perturbations, such as those resulting from rain events on urban stream microbiota. Here,  
28 we examined the microbial community composition and diversity in an urban stream during dry  
29 and wet weather conditions with both 16S rRNA gene sequencing across multiple years and  
30 shotgun metagenomics to more deeply analyze a single stormflow event. Metagenomics was  
31 used to assess population-level dynamics as well as shifts in the microbial community taxonomic  
32 profile and functional potential before and after a substantial rainfall. Results demonstrated  
33 general trends present in the stream under stormflow vs. baseflow conditions across years and  
34 seasons and also highlighted the significant influence of increased effluent flow following rain in  
35 shifting the stream microbial community from abundant freshwater taxa to those more associated  
36 with urban/anthropogenic settings. Shifts in the taxonomic composition were also linked to  
37 changes in functional gene content, particularly for transmembrane transport and organic  
38 substance biosynthesis. We also observed an increase in relative abundance of genes encoding  
39 degradation of organic pollutants and antibiotic resistance after rain. Overall, this study provided  
40 evidence of stormflow impacts on an urban stream microbiome from an environmental and  
41 public health perspective.

## 42 **Importance**

43 Urban streams in various parts of the world are facing increased anthropogenic pressure on their  
44 water quality, and stormflow events represent one such source of complex physical, chemical

45 and biological perturbations. Microorganisms are important components of these streams from  
46 both ecological and public-health perspectives, and analyzing the effect of such perturbations on  
47 the stream microbial community can help improve current knowledge on the impact such chronic  
48 disturbances can have on these water resources. This study examines microbial community  
49 dynamics during rain-induced stormflow conditions in an urban stream of the Chicago Area  
50 Waterway System. Additionally, using shotgun metagenomics we identified significant shifts in  
51 the microbial community composition and functional gene content following a high rainfall  
52 event, with potential environment and public health implications. Previous work in this area has  
53 been limited to specific genes/organisms or has not assessed immediate stormflow impact.

54

## 55 **Introduction**

56 Streams and rivers are important freshwater resources, used for recreation, agriculture, domestic  
57 water sources and industrial purposes. By storing, processing, and transporting terrestrially  
58 derived nutrients and organic matter, rivers play an important ecological role in linking  
59 biogeochemical cycles between terrestrial and aquatic ecosystems (1). Over the last century,  
60 many streams and rivers have witnessed rapid urbanization and anthropogenic development of  
61 their drainage basins, which has exposed them to frequent external inputs in the form of  
62 wastewater treatment plant (WWTP) effluent, industrial discharge, and sewer/stormwater  
63 overflows. These inputs often impact stream hydrological, physicochemical, and biological  
64 characteristics (2). For streams and rivers that serve as wastewater and/or stormwater outfall  
65 sites, rain-induced stormflow events are especially influential, as they often lead to an increased  
66 influx of WWTP effluent and unregulated waste via combined sewer overflows (CSOs) (3, 4).  
67 These perturbations bring in nutrients, a variety of microorganisms including pathogens, and

68 chemical pollutants such as steroid hormones that impact water quality, biodiversity, and  
69 ecosystem health (2, 3, 5, 6).

70 Because urban aquatic streams are typically highly variable systems that are regularly  
71 subject to anthropogenic inputs, it is unclear how much isolated perturbations such as rainfall  
72 and associated increases in stormflow might influence the water column microbial community,  
73 even in the short-term. Studies investigating urban river microbiota using genetic markers for  
74 fecal bacteria or 16S rRNA gene-based microbial community surveys have shown the presence  
75 of human fecal contamination, ‘urban signature’ bacteria and changes in community composition  
76 in streams and rivers impacted by WWTP effluent, stormwater, and CSOs (7–11). Moreover,  
77 others have documented the possible influx of antibiotic resistance bacteria and pathogens from  
78 WWTP effluent (12, 13) and stormwater events (6, 14) into urban environments, further  
79 signifying the importance of evaluating the persistence of these organisms and their impact on  
80 the riverine microbiome from a public health perspective. While these studies provide valuable  
81 information about the effects of stormflow events on urban stream microbial content they are  
82 limited to specific taxonomic and pollutant marker genes. Recent whole genome shotgun (WGS)  
83 metagenomics-based approaches have explored community composition and functional  
84 dynamics in urban impacted streams (15, 16), although a direct effect of stormflow on microbial  
85 dynamics remains less explored. A robust evaluation of the impacts of such isolated and short-  
86 term perturbations is critical for making predictions about the public health and possible longer-  
87 term ecological implications.

88 In this study, we used both 16S rRNA gene amplicon and shotgun metagenomics to  
89 deeply analyze the water column microbial community during baseflow and stormflow  
90 conditions in the North Shore Channel (NSC) stream, a section of the highly urbanized Chicago

91 Area Waterway System (CAWS) (Fig. S1). We focused on a site downstream of a WWTP and  
92 numerous CSO outflow points using 16S rRNA gene amplicon sequencing of samples from both  
93 baseflow and stormflow over the course of multiple seasons and years. Additionally, samples  
94 obtained immediately before and shortly (<24 hr) after a single rain event at the same site  
95 provided an opportunity for a deep analysis of short-term variability in the taxonomic and  
96 functional composition of the water-column microbiome using WGS metagenomics. Coupled  
97 with the 16S rRNA data from multiple samples, we were able to link some of these changes to  
98 stormflow conditions. We identified notable rainfall-induced changes in the stream microbial  
99 taxonomic and functional profiles, driven by shifts in the relative abundance of a few abundant  
100 microbial groups such as Actinobacteria and *Legionella* that could be functionally linked to the  
101 processes of transmembrane transport and organic substance biosynthesis. We also observed an  
102 increase in genes associated with antibiotic resistance and biodegradation of known wastewater  
103 pollutants following rain. Although our deep metagenomics-based analysis is centered around a  
104 single event, our findings provides a window into the variability and short-term changes in an  
105 urban freshwater system and sets the groundwork for making predictions about possible  
106 ecosystem level and public health related impacts of rainfall events on these systems. Overall,  
107 our results show that rain-associated WWTP effluent flow and perhaps CSOs impact the stream  
108 microbiome composition and functional potential, with the introduction of exogenous organisms  
109 to the system being a significant driver of the observed change.

110

## 111 **Results and Discussion**

### 112 *Impact of rainfall on North Shore Channel (NSC) microbial community composition*

113 Rainfall can impact urban waterways by increasing effluent flow from WWTPs or causing  
114 combined sewer overflow events (CSOs) at outflow points along streams (4). The NSC site that  
115 we investigated has a WWTP (O'Brien Water Reclamation Plant) and several CSO outfall sites  
116 within a few km upstream (Fig. S1) and often experiences increased flow from both following  
117 rainfall, including the two rain events reported in this study  
118 (<http://www.mwr.org/irj/portal/anonymous/overview>)(Fig. S2). Sequences from 16S rRNA  
119 gene amplicons at five distinct times between 2013-2015 representing both summer and fall and  
120 stream baseflow (dry weather; three samples) and stormflow (<24 hours after rain; two samples)  
121 (additional details are in Table S1) revealed both a seasonal/temporal and rainfall-associated  
122 clustering of the samples at the OTU level (PCoA, Bray-Curtis metric) (Fig. 1A). In particular,  
123 the separate clustering of stormflow and baseflow samples along the Principal Axis 2 highlights  
124 the strong influence of rain on the microbial community composition across different seasons.  
125 Such changes might result from either a direct influx of allochthonous microbes or a shift in the  
126 resident microbial community in response to altered chemical conditions following rain,  
127 although none of the measured physicochemical parameters showed a statistically significant  
128 difference between stormflow and baseflow conditions ( $p > 0.05$ , Welch's t-test; Table S1). In  
129 addition to shifts in community composition, microbial diversity based on OTU richness and  
130 Good's coverage was slightly higher in the stormflow samples than the baseflow samples (Table  
131 S2), although the differences were not significant ( $p > 0.05$ , Welch's t-test).

132 To analyze shifts in the microbial community across all stormflow vs. baseflow samples,  
133 OTUs were clustered at various hierarchical taxonomic levels. There was a difference in genus-  
134 based community composition between the stormflow and baseflow samples as per ANOSIM  
135 (Bray-Curtis metric,  $R^2 = 0.5$ ,  $p = 0.1$ ). Genus-level comparisons of microbial community

136 composition revealed a significantly lower abundance of unknown genera within groups  
137 *Pelagibacteraceae*, ACK-M1 and *Actinomycetales* and a significantly higher abundance of  
138 *Arcobacter* and unknown genera within the family *Rhodocyclaceae* during stormflow as  
139 compared to baseflow ( $p < 0.05$ , Welch's t-test) (Fig. 1B). The ACK-M1 family of  
140 Actinobacteria and *Pelagibacteraceae* are common freshwater organisms that do not favor  
141 nutrient rich conditions (17, 18) while genera within *Rhodocycleae* are Betaproteobacteria  
142 known to take advantage of nutrient/substrate-rich conditions, likely due to higher growth rates  
143 (17). *Rhodocycleae* has previously been associated with urban streams and was reported to be  
144 abundant in impacted Milwaukee waterways (19). Similarly, *Arcobacter* has often been  
145 associated with sewage and WWTP effluent (8, 9, 20). The increase in the relative abundance of  
146 these organisms in the NSC following rainfall could be due to point source inputs from the  
147 increased effluent flow and/or CSOs and was analyzed in more detail with shotgun  
148 metagenomics (see below).

149 Overall, the rain-associated changes in the microbial community composition appeared to  
150 be directly related to increased effluent; the after rain community OTUs were more similar to  
151 those in the WWTP effluent than to the before rain community (Fig. 1A). This could be linked to  
152 a few taxa, such as unknown genera within families *Procabacteriaceae* and *Legionellaceae* as  
153 well as the genus *Arcobacter*, which were abundant in the effluent and increased in the stream  
154 post-rain (Fig. 1B).

155

156 *Metagenomics-based microbial community composition before and after rain in North Shore*

157 *Channel*

158 The overall trends from the 16S rRNA gene-based analysis across seasons and years warranted a  
159 whole community metagenomic analysis of more temporally resolved samples clustered around  
160 a large rainfall event. Metagenomes with 4.06-16.21 million reads per library were obtained  
161 (Table S3) from the same NSC site discussed above (Fig. S1) before and <24 h after a heavy  
162 rainfall that followed a dry period in October 2013 (Fig. S2). These were used to  
163 comprehensively identify short-term changes in the microbial taxonomic profile after the rain.  
164 The rain resulted in increased WWTP effluent flow into the stream for ~24 h following  
165 precipitation, from <200 MGD to >300 MGD, and several CSO events at at-least three outfall  
166 locations upstream of sampled site within 10 h of rain  
167 (<http://www.mwrd.org/irj/portal/anonymous/overview>)(Fig. S2). Community coverage estimates  
168 using read redundancy (21) showed that the before rain metagenomes captured between 50-60%  
169 of the community and the after rain libraries captured approximately 40% (Fig. S3), indicating  
170 only a nominal increase in diversity after rainfall; a small increase in community OTU richness  
171 after rain was also observed with the 16S rRNA gene amplicon data (Table S2). Furthermore, the  
172 concentration of microbial cells in the before and after rain samples were similar:  $1.39 \times 10^6$  and  
173  $1.25 \times 10^6$  cells/ml, respectively. Previous studies have reported conflicting responses of microbial  
174 community diversity to urban inputs, with some showing an increase (20) and others a decrease  
175 (15, 23) relative to less impacted conditions/systems. This may be due to differing base  
176 conditions; the NSC is characterized by significant urban effluent flow even in the absence of  
177 rain. While Lake Michigan provides the primary freshwater input, about 70% of the annual flow  
178 through the CAWS is contributed by the treated effluent discharge from WWTPs in the city (24)  
179 during both baseflow and stormflow conditions. Our results do not show a strong pattern of  
180 change in microbial community diversity/richness during stormflow in NSC, perhaps because of



181 the variable nature of urban stream microbial communities or due to the small size of the this  
182 study. However, we hypothesize based on our results that individual rain events might not  
183 significantly impact microbial diversity in this system.

184 Despite overall similarities in microbial diversity and cell counts, numerous taxonomic  
185 differences were seen following rain, indicating that these changes likely reflect actual changes  
186 in microbial populations. The microbial communities pre- and post-rainfall determined both from  
187 16S rRNA genes and by assigning taxa to assembled metagenomic contigs showed overall  
188 concordance, however we focused on the assembled contigs for a high-resolution, population-  
189 level characterization of the community and to evaluate possible links between taxonomic and  
190 functional changes in the microbiome (24). About ~67% of the large (>500bp) contigs used by  
191 MyTaxa were classifiable at phylum level, ~35% at genus level, and 24% at species level. At the  
192 phylum level (Proteobacteria subdivided into classes), several individual taxa showed  
193 significantly different relative abundances after rain with large effect sizes (Fig. 2A).  
194 Actinobacteria and Bacteroidetes significantly decreased in relative abundance after rain whereas  
195 Gammaproteobacteria, Betaproteobacteria and Chlamydiae significantly increased ( $p < 0.05$ , t-  
196 test, false discovery rate corrected) (Fig. 2A). Similarity Percentage analysis (SIMPER, 26)  
197 revealed that Actinobacteria, Gammaproteobacteria and unclassified Proteobacteria contributed  
198 the most (35%, 14% and 21%, respectively) to the differences in community composition  
199 between the before and after rain samples at the phylum level. At the genus level, the decrease in  
200 relative abundance of Innominate (unclassified at genus level) Actinobacteria, *Candidatus*  
201 *Pelagibacter* and *Streptomyces* as well as the increase in relative abundance of *Legionella* and  
202 *Rickettsia*-affiliated sequences after rain contributed to the major change (>50%) in community  
203 composition (Fig. 2B). *Francisella*, *Nitrospira*, *Chlamydia* and *Pseudomonas* were other major

204 genera that increased significantly ( $p < 0.05$ , t-test, FDR corrected) in relative abundance in the  
205 after rain microbiome. As was observed with 16S rRNA amplicons in all samples (above), the  
206 urban signature bacteria *Arcobacter* increased by  $>50\%$  in relative abundance following rain,  
207 though the increase was not statistically significant (Fig. 2B). *Legionella*, *Pseudomonas* and  
208 *Arcobacter* have all been previously associated with effluent contamination of urban waterways  
209 (20), supporting the significant role of increased effluent flow on the NSC microbiome. Increases  
210 in the relative abundance of other taxa such as *Francisella*, *Rickettsia* and *Chlamydia* that  
211 comprise pathogenic species (27, 28) and are usually not abundant in aquatic environments could  
212 be either a result of microbial influx from the effluent and/or the CSOs upstream. The decrease  
213 in the freshwater groups of Actinobacteria and Pelagibacteria after rain likely reflects a dilution  
214 effect on baseflow NSC waters from the increased effluent and CSOs flow. Several species,  
215 including *Francisella tularensis*, *Candidatus Nitrospira defluvii*, *Legionella longbeachae* and  
216 *Enterococcus faecalis*, were rare ( $<0.1\%$  of the total sequences characterized by MyTaxa) in the  
217 before-rain microbiome but increased in relative abundance after rain to  $> 0.1\%$  (Table S3). Most  
218 of these species are not common freshwater bacteria and are indicative of contamination.

219

#### 220 Population-level changes in response to rainfall in the North Shore Channel

221 We followed population-level trends for abundant organisms that exhibited large changes in their  
222 relative abundance after rain. Organisms most similar to *Legionella pneumophila* increased 10-  
223 fold in relative abundance after rain and also comprised the largest fraction of characterized  
224 species (11%) in the after-rain microbiome. Reads were recruited to the longest contig assigned  
225 to *L. pneumophila* in the rain-associated samples with roughly equal similarity (about 90-100%  
226 nucleotide identity) from each sample, suggesting the presence of the same population both

227 before and after rain that increased substantially after rain (Fig. S4). This was supported by  
228 similarities in the average amino acid identity (AAI) of predicted protein coding genes from *L.*  
229 *pneumophila* before and after rainfall contigs (60% and 63%, respectively) to the genome  
230 sequences of the environmental isolate *L. pneumophila* strain LPE509 and the clinical isolate *L.*  
231 *pneumophila* subsp. *pneumophila* str. Philadelphia 1. The AAI between genes attributed to *L.*  
232 *pneumophila* in the before and after rain metagenomes was 83%. Although genome pairs for the  
233 same species typically exhibit higher AAIs (~90%) (29, 30), 83% still signifies close genetic  
234 relatedness and not necessarily distinct populations. Overall, these results indicate that the before  
235 and after rain *Legionella* are members of the same species, but different from any currently  
236 known, sequenced members of *Legionella*. The discordance between our *Legionella*-like  
237 organisms and well-characterized *L. pneumophila* strains also makes it unclear if the  
238 corresponding populations are pathogenic, although a few predicted genes (1 and 3 for the before  
239 and after rain metagenomes, respectively) had high identity matches (>90%) to known *L.*  
240 *pneumophila* virulence genes in the virulence factor database (<http://www.mgc.ac.cn/VFs/>).  
241 Organisms within *Legionella* have been associated with artificial aquatic environments such as  
242 water distribution systems and cooling towers in buildings (31, 32) as well as WWTP effluent  
243 (20), thus their dramatic post-rain surge is not surprising.

244 Another notable increase in relative abundance after rain (~16-fold) was attributed to  
245 *Francisella tularensis*, an organism with known soil- and water-borne pathogenic subspecies  
246 (26, 32). Using a similar approach as above, AAIs between genes attributed to *F. tularensis* in  
247 before and after rain samples and a reference genome of pathogenic subspecies *F. tularensis*  
248 subsp. *tularensis* SCHU S4 were 47% and 54%, respectively. Similar AAI values were observed  
249 between the metagenomic sequences and genomes of low virulent subspecies of this organism.

250 The AAI between the before and after rain *F. tularensis* genes was 68%. Thus, sequences  
251 classified as *F. tularensis* in our samples likely share the same taxonomic order Thiotrichales,  
252 but are different species from the known *F. tularensis* and might represent different populations  
253 within the same genus in the before and after rain samples, although the low number of  
254 sequences in the before rain dataset could bias in AAI calculation.

255 We also evaluated the population dynamics for species that dramatically dropped in  
256 relative abundance after the rain. *Actinobacterium* SCGC AAA027-L06 is a member of the  
257 ubiquitous freshwater *Actinobacteria* lineage acI-B (33), and the relative abundance of contigs  
258 affiliated with this organism decreased dramatically (43-fold) after rain. Read recruitment  
259 indicated similarity between the before and after rain populations, with reads from each sample  
260 sharing ~90-100% nucleotide identity to the largest contig of this organism, although fewer reads  
261 mapped to the contig from the after rain samples (Fig. S5). As with the *L. pneumophila*  
262 population, the 84% AAI between the before and after rain sequences indicates close genetic  
263 relatedness between the two populations. Furthermore, the AAIs with respect to the  
264 *Actinobacterium* SCGC AAA027-L06 draft genome were similar for the sequences from the  
265 before and after rain microbial communities (81% and 83%, respectively), indicating close  
266 genetic relatedness to this organism. Members of the acI-B lineage have been detected in diverse  
267 freshwater habitats (20, 35, 36, 38) and tend to prefer oligotrophic environments due to their  
268 small cell-size and oligotrophic life strategies (19, 36). Their decrease in relative abundance after  
269 rain likely reflects the reduced influence of freshwater flow from Lake Michigan due to  
270 increased wastewater flow.

271

272 Overall functional gene content in before and after rain microbial communities

273 Functional gene profiles revealed taxa-driven shifts in the microbial community functional  
274 potential after rain. Although many abundant Gene Ontology (GO) terms related to  
275 housekeeping functions, such as nucleic acid and small molecule binding, did not significantly  
276 change in relative abundance after rain (data not shown), we observed an increase of >50% of  
277 functions within the broad terms of transporter activity and carbohydrate metabolism after rain.  
278 These were primarily related to transmembrane and substrate-specific transporter activity and  
279 carbohydrate biosynthetic and metabolic processes, respectively (Fig. 3A). Genes related to  
280 multi-organism processes such as pathogenesis and conjugation were >50% more abundant after  
281 rain while the before-rain microbiome had >50% more functions related to catabolic process,  
282 amine metabolic process and phosphate containing compound metabolic process (Fig. 3A).  
283 Within the broad GOs, genes related to photosynthesis, biosynthesis of organic compounds such  
284 as amines, vitamins and pigments as well as the activity of enzyme groups oxidoreductase  
285 (acting on the CH-NH<sub>2</sub> group of donors) and ligase (forming phosphoric ester bonds) were twice  
286 as abundant in the before-rain microbiome (Fig. S6).

287         Within the broad GO term of transporter activity, genes related to substrate-specific  
288 transmembrane transporter activity, specifically organic acid and ion transmembrane transporter  
289 activity, doubled in relative abundance after rain from an average of 0.06% to an average of  
290 0.12% (Fig. S6). Genes encoding all transmembrane transporters were primarily attributed to  
291 Actinobacteria (31% of the identified sequences at phylum level) and unclassified Proteobacteria  
292 (22%) before rain, whereas unclassified Proteobacteria (39%) and Gammaproteobacteria (16%)  
293 were the major groups encoding transporters after rain (Fig. 3B). Gammaproteobacteria  
294 harboring transporter genes increased by 51% after rain while Actinobacteria encoding these  
295 genes exhibited more than 9-fold decrease, mirroring the shifts observed for the overall

296 taxonomic profiles for these groups (Fig. 2, 3B). Genera contributing to the increase in  
297 Gammaproteobacterial sequences included *Legionella*, *Francisella* and *Pseudomonas*, exhibiting  
298 a pattern similar to the shifts in their relative abundance in the overall microbial community.  
299 Furthermore, as with the overall microbial community, *Actinobacterium* SCGC AAA027-L06  
300 (unclassified at genus level) contributed the largest fraction of sequences encoding  
301 transmembrane transporter activity genes within Actinobacteria in the before rain community.  
302 Interestingly, based on the functional gene content of organisms with dominant shifts in their  
303 relative abundance, those organisms that increased after rain had a higher proportion of their  
304 genes affiliated to transporter functions compared to those that dropped in abundance after rain.  
305 For instance, 3.7% and 6.8% of the *L. pneumophila* and *F. tularensis* genes, respectively, were  
306 associated with transmembrane transport, whereas *Actinobacterium* SCGC AAA027-L06 and the  
307 genus *Pelagibacter* had  $\leq 2\%$ . Thus, the increase in transporter functions following the rain  
308 appears to be directly associated with an increase in the relative proportion of a subset of the  
309 organisms that harbor these functions rather than an increase in the distribution of these genes  
310 across the community. Organisms with transmembrane transporter genes, especially for organic  
311 substrates like organic acids, may be more suited to take advantage of the heterogeneous  
312 environment resulting from stormflow conditions.

313 Further evidence that changes in community composition drove the overall changes in the  
314 metabolic capacity came from genes that decreased in relative abundance after rain, such as  
315 those encoding biosynthesis of organic substances, which mirrored the overall shifts in taxa (Fig.  
316 2); Actinobacteria (39% of the identified sequences at phylum level) and unclassified  
317 Proteobacteria (31%) were the major taxa encoding organic substance biosynthesis before rain  
318 and unclassified Proteobacteria (45%) and Gammaproteobacteria (13%) after rain. The short-

319 term nature and lack of gene expression data makes it difficult to know about the viability and  
320 activity of these organisms, but taxa-driven shifts in community functional potential were  
321 recently observed in another river in response to sewage and terrestrial-derived organisms (15).

322

### 323 *Biodegradation and antibiotic resistance gene abundance before and after rain*

324 In addition to the GO-based functional analysis, we examined how rainfall impacted  
325 biodegradation and antibiotic resistance gene content. Predicted ORFs from both the before and  
326 after rain metagenomes were searched against a compiled database of protein sequences of  
327 microbial enzymes involved in the degradation of 12 different compounds associated with  
328 wastewater contamination, stormwater runoff, and WWTP effluent input (Fig. 4A). We detected  
329 biodegradation genes (BDGs) in both the before and after rain samples for 8 out of the 12  
330 contaminants tested, but observed a significant increase ( $p < 0.05$ , t-test) in the relative  
331 abundance of genes involved in the degradation of nicotine, phenol, 1,4-dichlorobenzene and  
332 pentachlorophenol and a decrease ( $p < 0.05$ ) in cholesterol degrading genes after rain (Fig. 4A).  
333 Additionally, the total relative abundance of all BDGs was significantly higher in the after rain  
334 sample ( $p < 0.05$ , t-test). BDGs before rain were primarily affiliated with unclassified  
335 Proteobacteria and Actinobacteria (35% and 30% of the identified sequences at phylum level,  
336 respectively), with the profile shifting to unclassified Proteobacteria and Betaproteobacteria  
337 (49% and 19%, respectively) as the dominant members of the community after rain, similar to  
338 the overall taxonomic shifts described above. These results reflect the increase in effluent flow  
339 from the WWTP as well as the suspected presence of these compounds in untreated wastewater  
340 and CSOs (3,38,40,42) (Fig. 4A).

341 Changes in the relative abundance of antibiotic resistance genes (ARGs) after rain were  
342 evaluated using the Comprehensive Antibiotic Resistance gene Database (CARD). As only a few  
343 ORFs (~10 per library) could be classified as ARGs from both the time points, we queried the  
344 unassembled paired-end reads against CARD. This resulted in several hits for various ARG  
345 categories in both time points (0.04% and 0.07% of the total number of reads for before and after  
346 rain samples, respectively) and revealed notable increases in the relative abundance of several  
347 ARG classes after rain (Fig. 4B), including significant increases in aminocoumarin and  
348 polymyxin resistance genes ( $p < 0.05$ , t-test). As with the BDGs, the total relative abundance for  
349 all ARGs pooled together for each time point was significantly higher in the after rain sample ( $p$   
350  $< 0.05$ , t-test). Increases in ARGs with urban-impacted stormflow was recently observed  
351 elsewhere as well (14), indicating that this could be a significant and underexplored effect of  
352 stormflow. Reads with high matches to ARGs were queried against metagenomic contigs,  
353 revealing that unclassified Proteobacteria and Firmicutes were the abundant ARG-carrying phyla  
354 (40% and 23% of the identified sequences at phylum level, respectively) in the before rain  
355 microbiome whereas unclassified Proteobacteria (50%) and Gammaproteobacteria (24%) were  
356 the dominant groups after the rain. This further supports the importance of taxa driven changes  
357 on gene content.

358 The results for both community composition and functional gene analysis provide  
359 evidence for the significant influence of WWTP effluent input on the microbial community,  
360 particularly from increased effluent flow-rates associated with heavy rain. Overall, this study  
361 revealed a shift in microbial community composition following rain from organisms frequently  
362 associated with freshwater systems towards organisms associated with urban impacted waters (9,  
363 20, 21) as well as a shift in functional gene content. The increased relative abundance (and



364 possibly actual abundance) of BDGs and ARGs along with the increase in genes associated with  
365 conjugation and pathogenesis in the after rain microbiome highlight the environmental and  
366 public health implications of stormflow in urban waterways. The extent to which these changes  
367 in gene content are expressed metabolically and persist is unknown. Although the WGS  
368 metagenomic analysis of a single rainfall event limits the scope of interpretations that can be  
369 drawn, our results provide substantial insights into microbial community dynamics in an urban  
370 stream during stormflow conditions, highlighting the need to investigate the urban stream  
371 microbiome with longer temporal scales and systematic sampling design to better predict the  
372 impact of rain associated stormflow events.

373

## 374 **Materials and Methods**

### 375 Site description and sample collection

376 The North Shore Channel (NSC) is a 12.3 km long man-made stream of the Chicago Area  
377 Waterway System that receives input from the O'Brien Water Reclamation Plant, a WWTP that  
378 serves over 1.3 million people residing in a 365 km<sup>2</sup> area and releases effluent into the NSC  
379 (<http://www.mwr.org/irj/portal/anonymous/waterreclamation>). Our study site is approximately  
380 1 km downstream of the WWTP outfall (Fig. S1). The NSC also has 48 CSOs along its course,  
381 six of which are located within about 1 km upstream of WWTP, and two are located within 1 km  
382 downstream of the WWTP. These release excess stormwater mixed with untreated sewage into  
383 the river when the transport and storage capacity of the city's sewage network is exceeded  
384 following high rainfall (<http://www.mwr.org/irj/portal/anonymous/overview>)(Fig. S1). Water  
385 from the selected NSC site was sampled five times between 2013-2015 (0-1 m depth): three  
386 represent stream water during base flow (dry weather) conditions, and the other two represent

387 stormflow (<24 hours after rainfall) conditions. We also sampled the WWTP effluent in October  
388 2013 during baseflow conditions. Additional sample metadata and water chemistry are in Table  
389 S1.

390 Water was collected using a horizontal sampler (Wildco, Yulee, FL, USA) and passed  
391 on-site in succession through ~1.6 µm pore size glass fiber filters to remove larger particles  
392 (Whatman, Pittsburgh, PA, USA) and collected on a 0.22 µm pore size polycarbonate membrane  
393 filters (EMD Millipore, Billerica, MA, USA). WWTP effluent was collected from the WWTP  
394 outlet where the released effluent mixes with stream water. About 10L of water was filtered in  
395 duplicate for each sample and ~20 ml of the filtrate was transported back to lab for chemical  
396 analysis. Water Temperature, pH, conductivity and total dissolved solids were measured on-site  
397 using a portable water quality meter (Hanna Instruments, Woonsocket, RI, USA). Additional  
398 water chemistry analysis is described in Table S1.

#### 399 DNA extraction and sequencing

400 DNA was extracted from filters as described in (46). Briefly, filters were incubated in lysis  
401 buffer (50 mM Tris-HCl, 40 mM EDTA, and 0.75 M sucrose) containing 1 mg/ml lysozyme and  
402 200 µg/ml RNase at 37 °C for 30 min. Subsequently, the samples were incubated with 1% SDS,  
403 10 mg/ml proteinase K at 55 °C and rotated overnight. From the lysate, DNA was extracted  
404 using phenol:chloroform, followed by ethanol precipitation and elution in TE buffer.

405 Whole genome shotgun (WGS) metagenomic sequencing was done on the Illumina  
406 HiSeq (v1) with paired end format and read length of 150 bp at the Michigan State University  
407 Research Technology Support Facility. We obtained 2.82 and 3.18 Gbp of paired-end read data  
408 for the before and after rain samples, respectively. Replicate filters were sequenced at the  
409 University of Illinois at Chicago DNA Services Facility (DNAS) on a single lane of the Illumina

410 HiSeq platform with paired end format and read length of 100 bp, yielding 4.04 and 1.31 Gbp of  
411 paired-end read data for the before and after rain libraries, respectively.

412 For 16S rRNA gene amplicon sequencing, 10-30 ng of DNA from each biological  
413 replicate (filter) were amplified with the V1-V3 primers 27F and 534R (47, 48). Amplicons were  
414 sequenced at the DNAS on the Illumina MiSeq platform with paired end format and read length  
415 of 300 bp. Between 28,933- 160,811 sequences per sample were obtained, with an average of  
416 61,337 sequences per sample. All these sequence data have been submitted to the Sequence Read  
417 Archive at NCBI under accession number SRP080963.

#### 418 16S rRNA gene based analysis of microbial community diversity

419 Paired-end barcoded reads of 16S rRNA gene amplicons were obtained for all the time points  
420 sampled and quality filtered using Trimmomatic (49) with a minimum average quality score of  
421 20 across a 4-base sliding window and a minimum read length of 100 bp (including primer) post  
422 trimming. Trimmed, paired-end reads were merged using Pear (50), but owing to low yield of the  
423 merged reads, likely due to issues related to the MiSeq V2 kit chemistry, further analysis was  
424 only performed on the trimmed forward reads. Reads were analyzed using QIIME version 1.8.0  
425 (51). Library statistics are summarized in Table S2. Chimeric sequences were removed using  
426 *identify\_chimeric\_seqs.py* with *usearch61* denovo method and *filter\_fasta.py*. Filtered sequences  
427 were clustered into operational taxonomic units (OTUs) at a 97% identity level using scripts  
428 *pick\_otus.py* and *pick\_rep\_set.py* based on *usearch61* denovo OTU picking. Representative  
429 OTUs were assigned taxonomy based on the Greengenes reference database (May 2013 version)  
430 using *assign\_taxonomy.py* with *uclust*. OTUs occurring as singletons or with sequences from just  
431 one library were excluded from analyses. Community taxonomic composition and alpha  
432 diversity was performed using *summarize\_taxa.py* and *alpha\_diversity.py*, respectively, with a

433 random subsample of 17,384 sequences per sample to avoid bias arising from variation in  
434 sequencing depth. Good's coverage for each library was estimated using *alpha\_diversity.py* and  
435 OTUs that included singletons, subsampled to an even depth of 18,289 sequences per library, the  
436 smallest library size.

#### 437 Metagenomic sequence assembly and phylogenetic classification

438 Raw metagenomic sequences were quality filtered using a Phred average per sliding window  
439 with quality threshold  $Q \geq 20$  and not allowing any N's. Quality filtered coupled reads for each  
440 metagenomic library were assembled as described in (46). Coupled reads were first assembled  
441 into contigs with Velvet (52) and SOAPdenovo2 (53) separately, and input to Newbler 2.0 to  
442 obtain longer contigs with better N50 values (54). Additional metagenomic library statistics are  
443 provided in Table S3. Gene calling was done with MetaGeneMark (55). Due to uneven data  
444 yields from sequencing, we used assemblies from the first sequencing run for each sample as the  
445 representative sequences for annotations, and mapped the coupled reads from both the replicate  
446 libraries to these contigs for each sample to calculate the contig coverage in each library. The  
447 predicted protein coding genes for each dataset were used for phylogenetic classification of the  
448 corresponding contigs using MyTaxa (28) with a database of all sequenced bacterial and archaeal  
449 genomes (<http://enve-omics.ce.gatech.edu/data/mytaxa>) using DIAMOND blastp in the sensitive  
450 mode (56). Reads were mapped to contigs using blastn with cutoffs  $\geq 50\%$  alignment length,  
451 identity  $\geq 97\%$  and e-value  $\leq 10^{-10}$ . Contig coverage (sum of lengths of reads mapping to  
452 contig/contig length) was used as a proxy for *in situ* abundance in each library and calculated  
453 using the *BlastTab.seqdepth\_nomedian.pl* script from the Enveomics bioinformatics toolbox  
454 (57). The script *aai.rb* from the same toolbox was used to calculate average amino acid identity  
455 (AAI) between any two sets of protein coding genes.

456 *Analysis of functional gene content and antibiotic resistance genes*

457 Predicted metagenomic genes were searched against the SwissProt database (58) using blastp  
458 and cutoffs of at least 40% sequence identity, 70% coverage of the query sequence and e-value  $\leq$   
459  $10^{-10}$ . The SwissProt match for the best hit for each query sequence was mapped to its  
460 corresponding Gene Ontology (GO) term (59), followed by binning the characterized genes at  
461 various depths (distance of a GO term from the parent node) of the GO database using in-house  
462 scripts. To evaluate the functional profile at a specific depth, *in situ* abundance for these GO  
463 terms was calculated using gene coverage (described above), and relative abundance for each  
464 GO term was obtained as a fraction of the total abundance of genes with identified functions in  
465 that library. The taxonomic affiliation of genes classified within a specific GO term was  
466 evaluated using MyTaxa, as described above.

467 To specifically evaluate the presence and abundance of genes involved in biodegradation  
468 of select wastewater contaminants in the rain-associated metagenomes, we created a database of  
469 protein sequences of enzymes related to degradation of select contaminants that are commonly  
470 found in WWTP effluent and sewage: testosterone; ibuprofen; caffeine; nicotine; cholesterol;  
471 1,4-dichlorobenzene; methyl-naphthalene; pentachlorophenol; phenol; N,N, diethyl-3-toluamide;  
472 tetrachloroethylene and phthalate (3, 38–43). The enzymes were selected based on their role in  
473 the degradation pathways for these compounds (60), as well as the sequence availability in  
474 NCBI. This database is available from the corresponding author upon request. The predicted  
475 ORFs were searched against this database using blastp and the best hits were filtered at same  
476 thresholds used for SwissProt (above). Coverage estimates were used for calculating the *in situ*  
477 abundance for each BDG class, and normalized for each library by dividing the abundance of

478 each BDG class by the total coverage of all predicted genes in that library and multiplying the  
479 result by 1 million to obtain gene count per million genes per library.

480 Antibiotic resistance genes in the rain-associated samples were identified by searching  
481 the predicted ORFs as well as paired-end metagenomic reads against the Comprehensive  
482 Antibiotic Resistance gene Database (CARD) (61) using blastp and blastx and a threshold of at  
483 least 80% sequence identity and 80% coverage of the query sequence (62, 63). Filtered reads for  
484 each library were binned into broad antibiotic resistance categories using the Resistance Gene  
485 Categories index file provided on CARD website (<http://arpcard.mcmaster.ca/>), and the read  
486 counts for each category were normalized for the library size as read count for ARG category per  
487 million reads per library.

#### 488 Microbial abundance estimation using fluorescence microscopy

489 October 2013 NSC samples were fixed with paraformaldehyde (1% final concentration) in  
490 triplicate and stored in 4°C. Samples were then vortexed and collected on 25 mm black  
491 polycarbonate filters (0.2 µm pore size) and stained with 5 µl of a 10 mg/ml DAPI (4',6-  
492 diamidino-2-phenylindole) working solution diluted in 10X phosphate buffered saline (PBS).  
493 Microbial cells were enumerated (three slides from three replicate samples per time point) with  
494 an epifluorescence microscope (Zeiss Axio Scope.A1).

#### 495 Statistical analyses

496 Analysis of Similarity (ANOSIM) and Similarity Percentage (SIMPER) analysis on 16S and  
497 metagenomic community composition datasets, respectively, was performed using the R vegan  
498 package (64). The Statistical Analysis of Metagenomic Profiles (STAMP) software package was  
499 used for t-tests to evaluate differentially abundant taxonomic groups among the 16S rRNA gene  
500 and metagenomic datasets (65), and with R to evaluate differentially abundant physicochemical

501 parameters, ARGs and BDGs. Principal Coordinate Analysis (PCoA, Bray Curtis metric) of  
502 OTUs (singletons removed and table subsampled to an even depth per sample) was performed  
503 with the Phyloseq package in R (66).

504

## 505 **Acknowledgements**

506 This work was supported by the University of Illinois at Chicago. We thank Markeia Scruggs  
507 and Neil Mohindra for assistance with sampling and the personnel of the University of Illinois at  
508 Chicago DNA Services Facility for facilitating sample sequencing. We also thank the  
509 anonymous reviewers whose suggestions improved this manuscript.

510

## 511 **References**

- 512 1. **Cole JJ, Prairie YT, Caraco NF, McDowell WH, Tranvik LJ, Striegl RG, Duarte**  
513 **CM, Kortelainen P, Downing JA, Middelburg JJ, Melack J.** 2007. Plumbing the  
514 Global Carbon Cycle : Integrating Inland Waters into the Terrestrial Carbon Budget.  
515 *Ecosystems* **10**:171–184.
- 516 2. **Paul MJ, Meyer JL.** 2001. Streams in the urban landscape. *Annu Rev Ecol Syst* **32**:333–  
517 365.
- 518 3. **Phillips PJ, Chalmers a. T, Gray JL, Kolpin DW, Foreman WT, Wall GR.** 2012.  
519 Combined sewer overflows: An environmental source of hormones and wastewater  
520 micropollutants. *Environ Sci Technol* **46**:5336–5343.
- 521 4. **Weyrauch P, Matzinger A, Pawlowsky-Reusing E, Plume S, von Seggern D,**  
522 **Heinzmann B, Schroeder K, Rouault P.** 2010. Contribution of combined sewer  
523 overflows to trace contaminant loads in urban streams. *Water Res* **44**:4451–4462.
- 524 5. **Walsh CJ, Roy AH, Feminella JW, Cottingham PD, Groffman PM, Morgan II RP.**  
525 2005. The urban stream syndrome : current knowledge and the search for a cure. *J North*  
526 *Am Benthol Soc* **24**:706–723.
- 527 6. **Rechenburg A, Koch C, Claßen T, Kistemann T.** 2006. Impact of sewage treatment  
528 plants and combined sewer overflow basins on the microbiological quality of surface  
529 water. *Water Sci Technol* **54**:95–99.



- 530 7. **Sercu B, Werfhorst LC Van De, Murray J, Holden PA.** 2009. Storm drains are sources  
531 of human fecal pollution during dry weather in three urban Southern California  
532 watersheds. *Environ Sci Technol* **43**:293–298.
- 533 8. **Newton RJ, Bootsma MJ, Morrison HG, Sogin ML, McLellan SL.** 2013. A microbial  
534 signature approach to identify fecal pollution in the waters off an urbanized coast of Lake  
535 Michigan. *Microb Ecol* **65**:1011–1023.
- 536 9. **Fisher JC, Newton RJ, Dila DK, McLellan SL.** 2015. Urban microbial ecology of a  
537 freshwater estuary of Lake Michigan. *Elem Sci Anthr* **3**:000064.
- 538 10. **Drury B, Rosi-Marshall E, Kelly JJ.** 2013. Wastewater treatment effluent reduces the  
539 abundance and diversity of benthic bacterial communities in urban and suburban rivers.  
540 *Appl Environ Microbiol* **79**:1897–1905.
- 541 11. **Drury B, Scott J, Rosi-Marshall EJ, Kelly JJ.** 2013. Triclosan exposure increases  
542 triclosan resistance and influences taxonomic composition of benthic bacterial  
543 communities. *Environ Sci Technol* **47**:8923–8930.
- 544 12. **Czekalski N, Berthold T, Caucci S, Egli A, Bürgmann H.** 2012. Increased levels of  
545 multiresistant bacteria and resistance genes after wastewater treatment and their  
546 dissemination into Lake Geneva, Switzerland. *Front Microbiol* **3**:1–18.
- 547 13. **Rizzo L, Manaia C, Merlin C, Schwartz T, Dagot C, Ploy MC, Michael I, Fatta-  
548 Kassinos D.** 2013. Urban wastewater treatment plants as hotspots for antibiotic resistant  
549 bacteria and genes spread into the environment: A review. *Sci Total Environ* **447**:345–  
550 360.
- 551 14. **Zhang S, Pang S, Wang PF, Wang C, Han N, Liu B, Han B, Li Y, Anim-Larbi K.**  
552 2016. Antibiotic concentration and antibiotic-resistant bacteria in two shallow urban lakes  
553 after stormwater event. *Environ Sci Pollut Res* **23**:9984–9992.
- 554 15. **Meziti A, Tsementzi D, Ar. Kormas K, Karayanni H, Konstantinidis KT.** 2016.  
555 Anthropogenic effects on bacterial diversity and function along a river-to-estuary gradient  
556 in Northwest Greece revealed by metagenomics. *Environ Microbiol* **18**:4640–4652.
- 557 16. **Jeffries TC, Schmitz Fontes ML, Harrison DP, Van-Dongen-Vogels V, Eyre BD,  
558 Ralph PJ, Seymour JR.** 2016. Bacterioplankton dynamics within a large  
559 anthropogenically impacted urban estuary. *Front Microbiol* **6**:1–17.
- 560 17. **Newton RJ, Jones SE, Eiler A, McMahon KD, Bertilsson S.** 2011. A guide to the  
561 natural history of freshwater lake bacteria. *Microbiol Mol Biol Rev* **75**:14-49.
- 562 18. **Ghai R, Mizuno CM, Picazo A, Camacho A, Rodriguez-Valera F.** 2014. Key roles for  
563 freshwater Actinobacteria revealed by deep metagenomic sequencing. *Mol Ecol* **23**:6073–  
564 6090.



- 565 19. **Newton RJ, McLellan SL.** 2015. A unique assemblage of cosmopolitan freshwater  
566 bacteria and higher community diversity differentiate an urbanized estuary from  
567 oligotrophic Lake Michigan. *Front Microbiol* **6**:1–13.
- 568 20. **McLellan SL, Fisher JC, Newton RJ.** 2015. The microbiome of urban waters. *Int*  
569 *Microbiol* **18**:141–149.
- 570 21. **Rodriguez-R LM, Konstantinidis KT.** 2014. Nonpareil: A redundancy-based approach  
571 to assess the level of coverage in metagenomic datasets. *Bioinformatics* **30**:629–635.
- 572 22. **Kirs M, Kisand V, Wong M, Caffaro-Filho R a., Moravcik P, Harwood VJ,**  
573 **Yoneyama B, Fujioka RS.** 2017. Multiple lines of evidence to identify sewage as the  
574 cause of water quality impairment in an urbanized tropical watershed. *Water Res* **116**:23–  
575 33.
- 576 23. **Illinois Department of Natural Resources.** 2011. Illinois Coastal Management Program  
577 issue paper: Chicago River and North Shore Channel corridors. Illinois Department of  
578 Natural Resources, Springfield, IL, USA.
- 579 24. **Poretsky R, Rodriguez-R LM, Luo C, Tsementzi D, Konstantinidis KT.** 2014.  
580 Strengths and limitations of 16S rRNA gene amplicon sequencing in revealing temporal  
581 microbial community dynamics. *PLoS One* **9**:e93827.
- 582 25. **Clarke KR.** 1993. Non-parametric multivariate analyses of changes in community  
583 structure. *Aust J Ecol* **18**:117–143.
- 584 26. **Kingry LC, Petersen JM.** 2014. Comparative review of *Francisella tularensis* and  
585 *Francisella novicida*. *Front Cell Infect Microbiol* **4**:35.
- 586 27. **Stratton CW, Mitchell WM.** 1996. The pathogenesis of *Chlamydia* species.  
587 *Antimicrobics and Infectious Diseases Newsletter* **15**:83-88.
- 588 28. **Luo C, Rodriguez-R LM, Konstantinidis KT.** 2014. MyTaxa: An advanced taxonomic  
589 classifier for genomic and metagenomic sequences. *Nucleic Acids Res* **42**:e73.
- 590 29. **Rodriguez-R LM, Konstantinidis KT.** 2014. Bypassing cultivation to identify bacterial  
591 species. *Microbe* **9**:111–118.
- 592 30. **World Health Organization.** 2007. *In* Bartram J, Chartier Y, Lee JV, Pond K, Surman-  
593 Lee S (ed), *Legionella and the prevention of legionellosis*. WHO Press, Geneva,  
594 Switzerland.
- 595 31. **Lee HK, Shim JI, Kim HE, Yu JY, Kang YH.** 2010. Distribution of *Legionella* species  
596 from environmental water sources of public facilities and genetic diversity of *L.*  
597 *pneumophila* serogroup 1 in South Korea. *Appl Environ Microbiol* **76**:6547–6554.

- 598 32. **Petersen JM, Mead PS, Schriefer ME.** 2009. *Francisella tularensis*: An arthropod-borne  
599 pathogen. *Vet Res* **40**:07.
- 600 33. **Garcia SL, McMahon KD, Martinez-Garcia M, Srivastava A, Sczyrba A,**  
601 **Stepanaukas R, Grossart H, Woyke T, Warnecke F.** 2013. Metabolic potential of a  
602 single cell belonging to one of the most abundant lineages in freshwater bacterioplankton.  
603 *ISME J* **7**:137–147.
- 604 34. **Warnecke F, Amann R, Pernthaler J.** 2004. Actinobacterial 16S rRNA genes from  
605 freshwater habitats cluster in four distinct lineages. *Environ Microbiol* **6**:242–253.
- 606 35. **Ghai R, Rodríguez-Valera F, McMahon KD, Toyama D, Rinke R, de Oliveira TCS,**  
607 **Garcia JW, de Miranda FP, Henrique-Silva F.** 2011. Metagenomics of the water  
608 column in the pristine upper course of the Amazon river. *PLoS One* **6**:e23785.
- 609 36. **Ghylin TW, Garcia SL, Moya F, Oyserman BO, Schwientek P, Forest KT, Mutschler**  
610 **J, Dwulit-Smith J, Chan LK, Martinez-Garcia M, Sczyrba a, Stepanaukas R,**  
611 **Grossart HP, Woyke T, Warnecke F, Malmstrom R, Bertilsson S, McMahon KD.**  
612 2014. Comparative single-cell genomics reveals potential ecological niches for the  
613 freshwater acI Actinobacteria lineage. *ISME J* **8**:2503–2516.
- 614 37. **Satinsky BM, Fortunato CS, Doherty M, Smith CB, Sharma S, Ward ND, Krusche A**  
615 **V, Yager PL, Richey JE, Moran MA, Crump BC.** 2015. Metagenomic and  
616 metatranscriptomic inventories of the lower Amazon River, May 2011. *Microbiome* **3**:39.
- 617 38. **Boyd GR, Palmeri JM, Zhang S, Grimm DA.** 2004. Pharmaceuticals and personal care  
618 products (PPCPs) and endocrine disrupting chemicals (EDCs) in stormwater canals and  
619 Bayou St. John in New Orleans, Louisiana, USA. *Sci Total Environ* **333**:137–148.
- 620 39. **Glassmeyer ST, Furlong ET, Kolpin DW, Cahill JD, Zaugg SD, Werner SL, Meyer**  
621 **MT, Kryak DD.** 2005. Transport of chemical and microbial compounds from known  
622 wastewater discharges: Potential for use as indicators of human fecal contamination.  
623 *Environ Sci Technol* **39**:5157–5169.
- 624 40. **Benotti MJ, Brownawell BJ.** 2007. Distributions of pharmaceuticals in an urban estuary  
625 during both dry- and wet-weather conditions. *Environ Sci Technol* **41**:5795–5802.
- 626 41. **Phillips P, Chalmers A.** 2009. Wastewater effluent, combined sewer overflows, and other  
627 sources of organic compounds to Lake Champlain. *J Am Water Resour Assoc* **45**:45–57.
- 628 42. **Sauvé S, Aboufadel K, Dorner S, Payment P, Deschamps G, Prévost M.** 2012. Fecal  
629 coliforms, caffeine and carbamazepine in stormwater collection systems in a large urban  
630 area. *Chemosphere* **86**:118–23.

- 631 43. **Fang H, Cai L, Yu Y, Zhang T.** 2013. Metagenomic analysis reveals the prevalence of  
632 biodegradation genes for organic pollutants in activated sludge. *Bioresour Technol*  
633 **129**:209–218.
- 634 44. **Rechenburg a, Koch C, ClaBen T, Kistemann T.** 2006. Impact of sewage treatment  
635 plants and combined sewer overflow basins on the microbiological quality of surface  
636 water. *Water Sci Technol* **54**:95–99.
- 637 45. **Sidhu JPS, Ahmed W, Gernjak W, Aryal R, McCarthy D, Palmer A, Kolotelo P,**  
638 **Toze S.** 2013. Sewage pollution in urban stormwater runoff as evident from the  
639 widespread presence of multiple microbial and chemical source tracking markers. *Sci*  
640 *Total Environ* **463-464**:488–496.
- 641 46. **Oh S, Caro-Quintero A, Tsementzi D, DeLeon-Rodriguez N, Luo C, Poretsky R,**  
642 **Konstantinidis KT.** 2011. Metagenomic insights into the evolution, function, and  
643 complexity of the planktonic microbial community of Lake Lanier, a temperate freshwater  
644 ecosystem. *Appl Environ Microbiol* **77**:6000–6011.
- 645 47. **Frank JA, Reich CI, Sharma S, Weisbaum JS, Wilson B a., Olsen GJ.** 2008. Critical  
646 evaluation of two primers commonly used for amplification of bacterial 16S rRNA genes.  
647 *Appl Environ Microbiol* **74**:2461–2470.
- 648 48. **Somenahally AC, Mosher JJ, Yuan T, Podar M, Phelps TJ, Brown SD, Yang ZK,**  
649 **Hazen TC, Arkin AP, Palumbo A V., Van Nostrand JD, Zhou J, Elias DA.** 2013.  
650 Hexavalent chromium reduction under fermentative conditions with lactate stimulated  
651 native microbial communities. *PLoS One* **8**:e83909.
- 652 49. **Bolger AM, Lohse M, Usadel B.** 2014. Trimmomatic: A flexible trimmer for Illumina  
653 sequence data. *Bioinformatics* **30**:2114–2120.
- 654 50. **Zhang J, Kobert K, Flouri T, Stamatakis A.** 2014. PEAR: A fast and accurate Illumina  
655 Paired-End reAd mergeR. *Bioinformatics* **30**:614–620.
- 656 51. **Caporaso JG, Kuczynski J, Stombaugh J, Bittinger K, Bushman FD, Costello EK,**  
657 **Fierer N, Peña AG, Goodrich JK, Gordon JI, Huttley GA, Kelley ST, Knights D,**  
658 **Koenig JE, Ley RE, Lozupone CA, McDonald D, Muegge BD, Pirrung M, Reeder J,**  
659 **Sevinsky JR, Turnbaugh PJ, Walters WA, Widmann J, Yatsunenko T, Zaneveld J,**  
660 **Knight R.** 2010. QIIME allows analysis of high-throughput community sequencing data.  
661 *Nat Methods* **7**:335–6.
- 662 52. **Zerbino DR, Birney E.** 2008. Velvet: Algorithms for de novo short read assembly using  
663 de Bruijn graphs. *Genome Res* **18**:821–829.
- 664 53. **Luo R, Liu B, Xie Y, Li Z, Huang W, Yuan J, He G, Chen Y, Pan Q, Liu Y, Tang J,**  
665 **Wu G, Zhang H, Shi Y, Liu Y, Yu C, Wang B, Lu Y, Han C, Cheung DW, Yiu S-M,**  
666 **Peng S, Xiaoqian Z, Liu G, Liao X, Li Y, Yang H, Wang J, Lam T-W, Wang J.** 2012.

- 667 SOAPdenovo2: an empirically improved memory-efficient short-read de novo assembler.  
668 *Gigascience* **1**:18.
- 669 54. **Luo C, Tsementzi D, Kyrpides NC, Konstantinidis KT.** 2012. Individual genome  
670 assembly from complex community short-read metagenomic datasets. *ISME J* **6**:898–901.
- 671 55. **Zhu W, Lomsadze A, Borodovsky M.** 2010. Ab initio gene identification in  
672 metagenomic sequences. *Nucleic Acids Res* **38**:e132.
- 673 56. **Buchfink B, Xie C, Huson DH.** 2015. Fast and sensitive protein alignment using  
674 DIAMOND. *Nat Methods* **12**:59–60.
- 675 57. **Rodriguez-R LM, Konstantinidis KT.** 2016. The enveomics collection : a toolbox for  
676 specialized analyses of microbial genomes and metagenomes. *Peer J Prepr* **4**:e1900v1.
- 677 58. **Wu CH, Apweiler R, Bairoch A, Natale D a, Barker WC, Boeckmann B, Ferro S,  
678 Gasteiger E, Huang H, Lopez R, Magrane M, Martin MJ, Mazumder R, O'Donovan  
679 C, Redaschi N, Suzek B.** 2006. The Universal Protein Resource (UniProt): an expanding  
680 universe of protein information. *Nucleic Acids Res* **34**:D187–91.
- 681 59. **Ashburner M, Ball CA, Blake JA, Botstein D, Butler H, Cherry JM, Davis AP,  
682 Dolinski K, Dwight SS, Eppig JT, Harris MA, Hill DP, Issel-Tarver L, Kasarskis A,  
683 Lewis S, Matese JC, Richardson JE, Ringwald M, Rubin GM, Sherlock G.** 2000.  
684 Gene Ontology: tool for the unification of biology. *Nat Genet* **25**:25–29.
- 685 60. **Gao J, Ellis LBM, Wackett LP.** 2009. The University of Minnesota  
686 Biocatalysis/Biodegradation Database: Improving public access. *Nucleic Acids Res*  
687 **38**:488–491.
- 688 61. **McArthur AG, Waglechner N, Nizam F, Yan A, Azad M a., Baylay AJ, Bhullar K,  
689 Canova MJ, De Pascale G, Ejim L, Kalan L, King AM, Koteva K, Morar M, Mulvey  
690 MR, O'Brien JS, Pawlowski AC, Piddock LJ V, Spanogiannopoulos P, Sutherland  
691 AD, Tang I, Taylor PL, Thaker M, Wang W, Yan M, Yu T, Wright GD.** 2013. The  
692 comprehensive antibiotic resistance database. *Antimicrob Agents Chemother* **57**:3348–  
693 3357.
- 694 62. **Gibson MK, Forsberg KJ, Dantas G.** 2014. Improved annotation of antibiotic resistance  
695 determinants reveals microbial resistomes cluster by ecology. *ISME J* **9**:1–10.
- 696 63. **Port JA, Cullen AC, Wallace JC, Smith MN, Faustman EM.** 2014. Metagenomic  
697 frameworks for monitoring antibiotic resistance in aquatic environments. *Environ Health*  
698 *Perspect* **122**:222–228.
- 699 64. **Oksanen J, Blanchet FG, Kindt R, Legendre P, Minchin PR, O'Hara RB, Simpson  
700 GL, Solymos P, Stevens MHH, Wagner H.** 2015. vegan: Community Ecology Package.  
701 R package version 2.2-1. <http://CRANR-project.org/package=vegan>.

702 65. **Parks DH, Tyson GW, Hugenholtz P, Beiko RG.** 2014. STAMP: Statistical analysis of  
703 taxonomic and functional profiles. *Bioinformatics* **30**:3123–3124.

704 66. **McMurdie PJ, Holmes S.** 2013. Phyloseq: An R Package for Reproducible Interactive  
705 Analysis and Graphics of Microbiome Census Data. *PLoS One* **8**:e61217.

706

## 707 **Supplemental Table and Figure Legends**

708 **Table S1:** Water chemistry and environmental characteristics for North Shore Channel sampled  
709 time points.

710 **Table S2:** Sequencing statistics and diversity estimates for the 16S rRNA gene amplicon  
711 libraries used in the study.

712 **Table S3:** Sequencing statistics for the metagenomes used in the study.

713 **Table S4:** Rare species in before rain microbiome that were in the abundant fraction after rain.

714 **Fig. S1:** Map of the Chicago Area Waterway System (left panel) and the North Shore Channel  
715 (NSC) (right panel). Our study site at NSC is highlighted with an arrow. The point designated as  
716 WWTP on the right panel represents the O'Brien Water Reclamation Plant. Black dots along the  
717 stream represent locations for monitored CSO outfalls. CSO outfalls marked with red stars  
718 (locations A, B and C) recorded CSO events in the evening of Oct 5, 2013 with durations of 56,  
719 50 and 5 minutes, respectively (<http://www.mwrd.org/irj/portal/anonymous/overview>).

720 **Fig. S2:** O'Brien Water Reclamation Plant effluent flow rate [million gallons per day (MGD)]  
721 and rain gauge data for the months of September and October 2013  
722 (<http://www.mwrd.org/irj/portal/anonymous/overview>). The circled region of the plot  
723 corresponds to data around the rain event (10/5/2013), which is the focus of this study. No data  
724 was available for 9/17/2013 as the rain gauge was out of service.

725 **Fig. S3:** Community coverage estimates based on metagenomic reads generated using Nonpareil  
726 for the before and after rain metagenomes. Sample numbers 1 and 2 for each time point represent  
727 biological replicate libraries.

728 **Fig. S4:** Reads from before rain (top) and after rain (bottom) datasets were mapped to the longest  
729 contig attributed to *Legionella pneumophila* from the after rain metagenome. Reads for  
730 biological replicate libraries (n= 2) were pooled for both the before and after rain time points.

731 **Fig. S5:** Reads from before rain (top) and after rain (bottom) datasets were mapped to the longest  
732 contig attributed to *Actinobacterium SCGC AAA027-L06* from the before rain metagenome.  
733 Reads for biological replicate libraries (n= 2) were pooled for both the before and after rain time  
734 points.

735 **Fig. S6:** Heat map showing the relative abundance (percentage of total predicted genes) at level  
736 4 depth of Gene Ontology (GO) terms for the before and after rain microbiomes. GO terms that  
737 had a higher relative abundance (> 100%) in one of the two groups (before/after rain) as  
738 compared to the other are shown, and terms that had less than a total of 75 gene counts across all  
739 the samples have been excluded from the plot. Samples numbered 1 and 2 for each time point  
740 represent biological replicates.

741

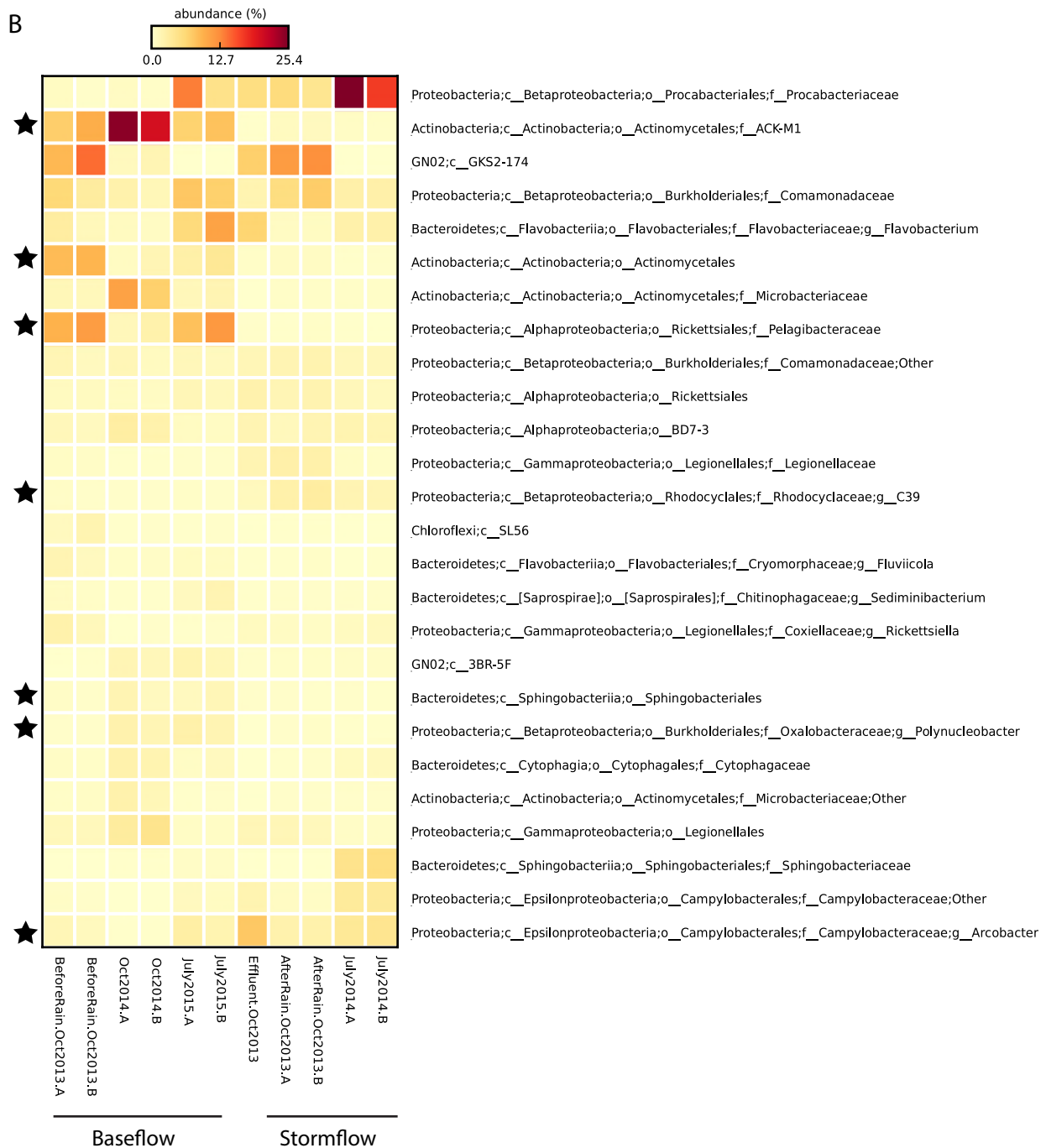
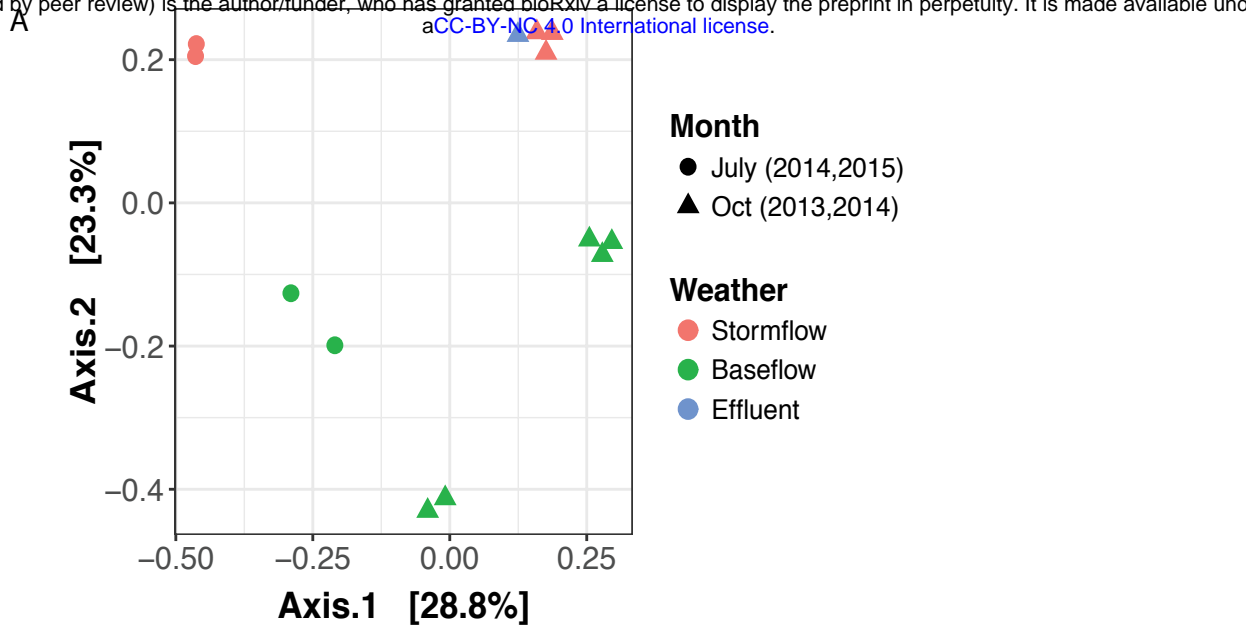
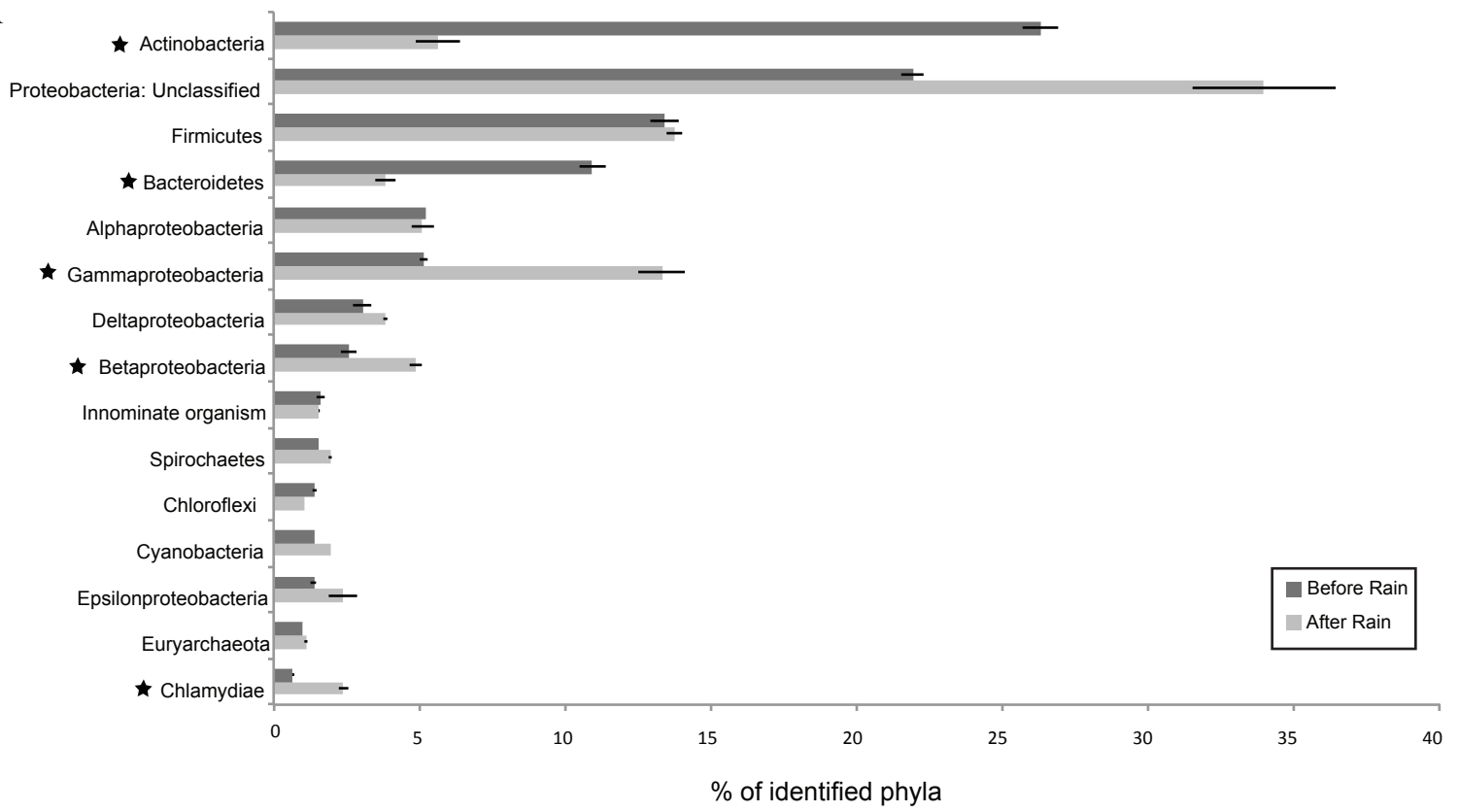




**Figure 1: (A)** Principal coordinate analysis (PCoA) (Bray-Curtis metric) of OTU-based microbial community diversity for North Shore Channel (NSC) water and WWTP effluent. Samples were obtained during either baseflow or stormflow conditions between 2013-2015 in summer (July) and fall (October) seasons. Each NSC time point is represented on the PCoA by biological duplicates, except for Oct-2013 stormflow and baseflow samples that also have sequencing duplicates for one of their bio-samples. **(B)** Heat map representing the relative abundance (percent of total 16S rRNA gene sequences) of dominant bacterial taxa classified till the lowest possible level (up-to genus) for the NSC and effluent samples. Taxa highlighted with a star symbol represent bacterial groups with significantly different relative abundance ( $p < 0.05$ , Welch's t-test) between the stormflow and baseflow samples of NSC. Two biological replicates marked as A and B represent each NSC time point, and the average value of these replicates per time point was used in Welch's t-test between the two groups (stormflow and baseflow).



A



B

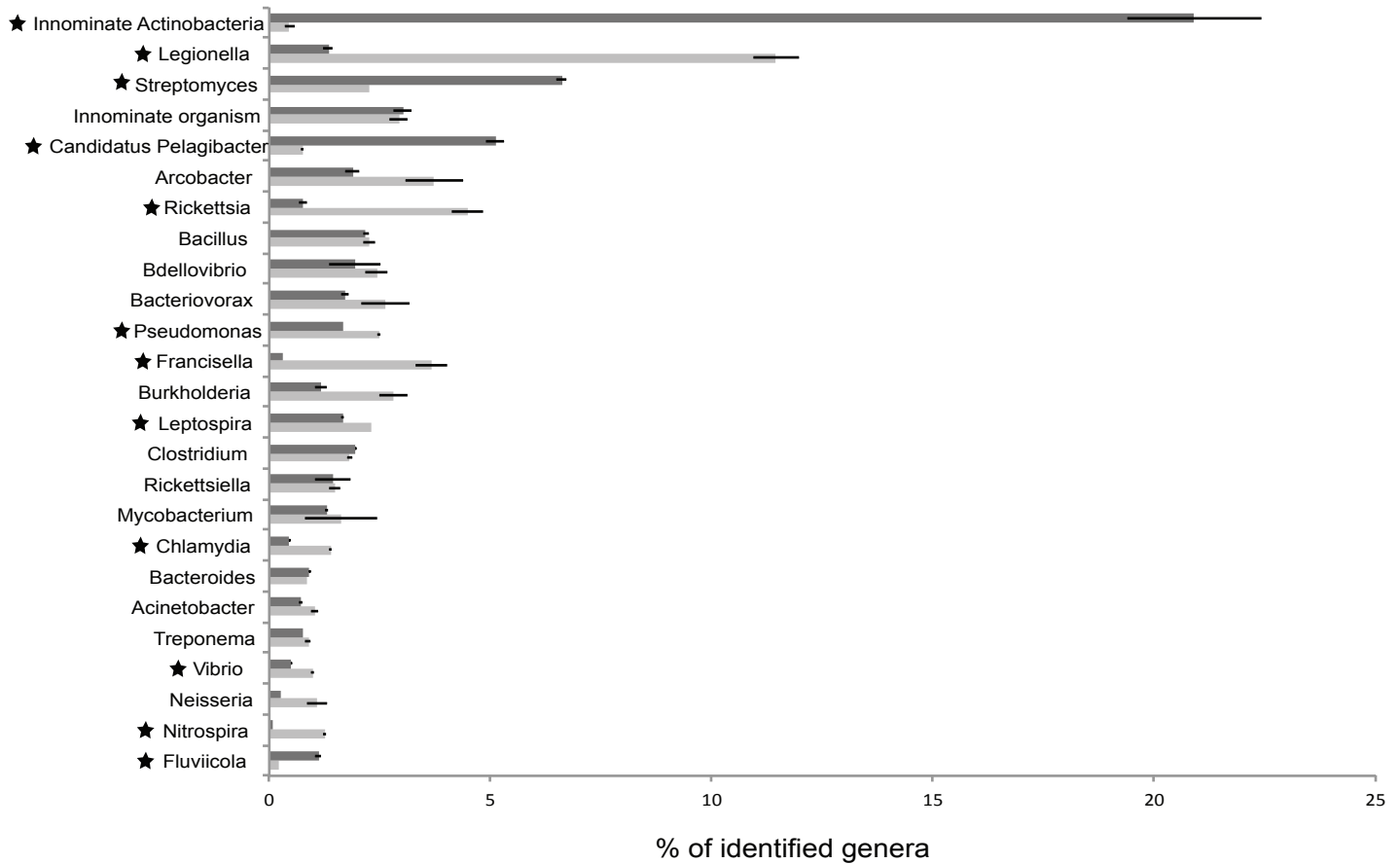
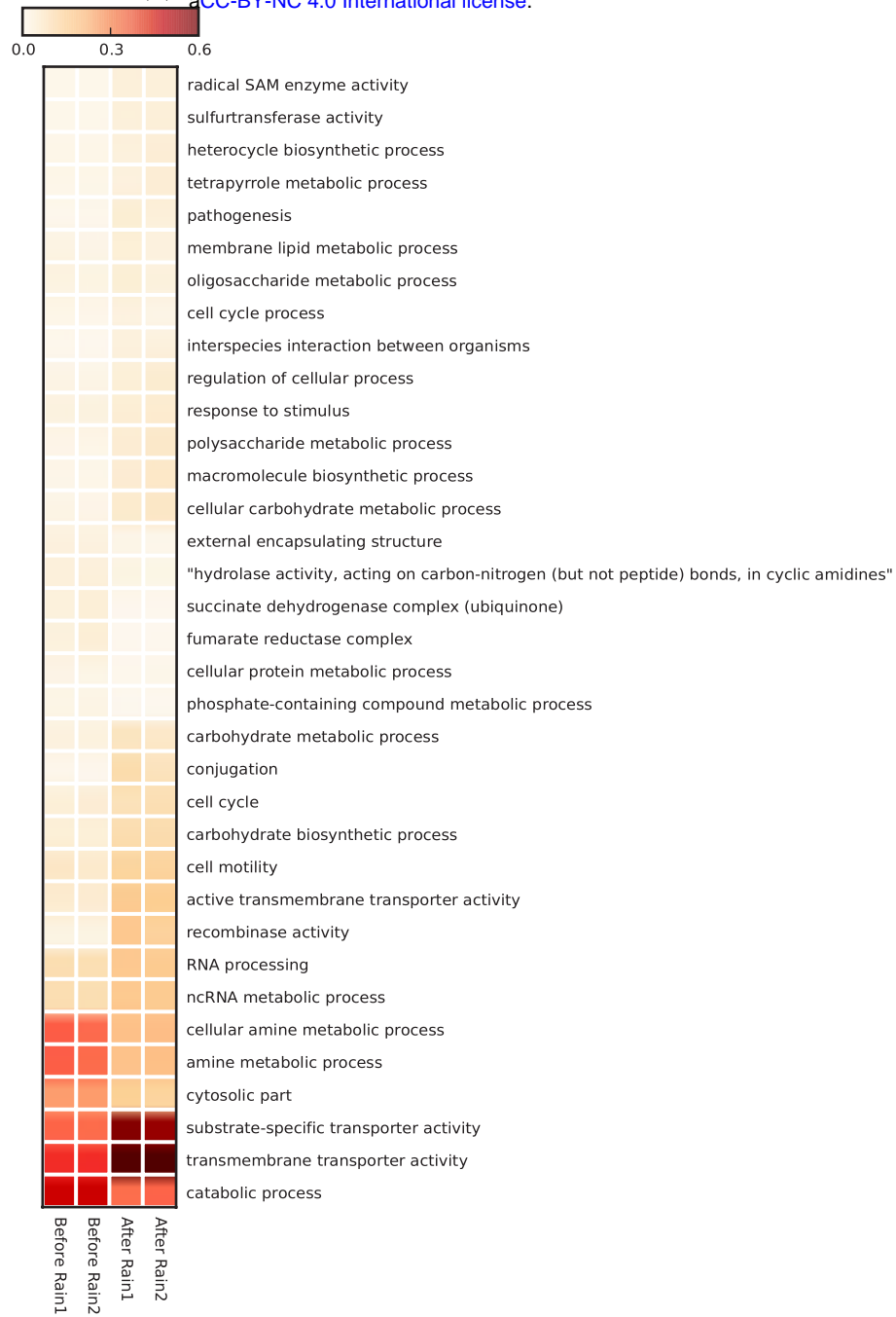


**Figure 2:** Rank-abundance plots for (A) phylum (Proteobacteria subdivided into classes) and (B) genus level classifications of metagenomic contigs from October 2013 before and after rain samples. The relative abundances of different taxa are averages of biological replicates for each sample (n=2). Based on taxon mean relative abundance across the samples, only the top 15 phyla and top 25 genera are shown. Phyla and genera highlighted with star symbol represent taxa with significant difference in relative abundance between the before and after rain microbiota ( $p < 0.05$ , t-test, false discovery rate corrected). ‘Innominate organism’ comprises contigs classified as organisms that either belonged to no known phylum/genus or a candidate phylum/genus.

A



B

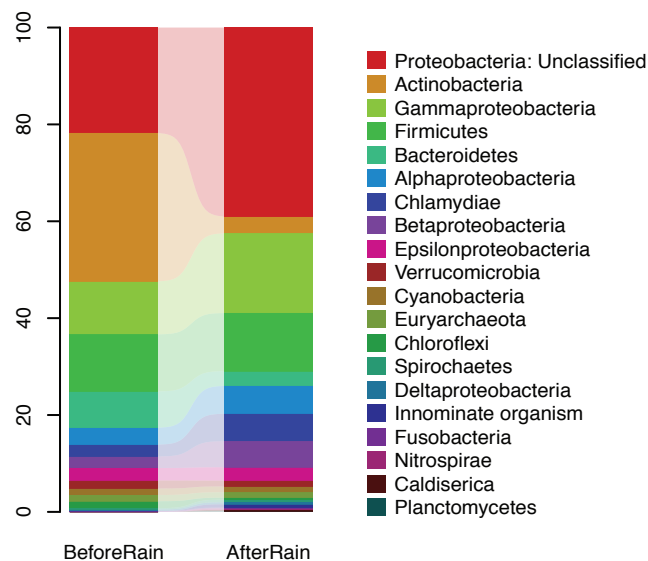


**Figure 3: (A)** Heatmap showing relative abundance (percentage of total predicted genes) at level 3 of Gene Ontology (GO) terms for the before and after rain microbiomes. GOs that had a higher relative abundance (> 50%) in one of the two groups (before/after rain) as compared to the other are shown. GOs that had less than 100 gene counts (*in situ* abundance) across all the samples have been excluded from the plot. Samples numbered 1 and 2 for each time point represent biological replicates. **(B)** Taxonomic composition at phylum level of genes from the rain-event microbial communities classified within the GO term ‘transmembrane transporter activity’. Relative abundances are a fraction of total sequences identified at phylum level.

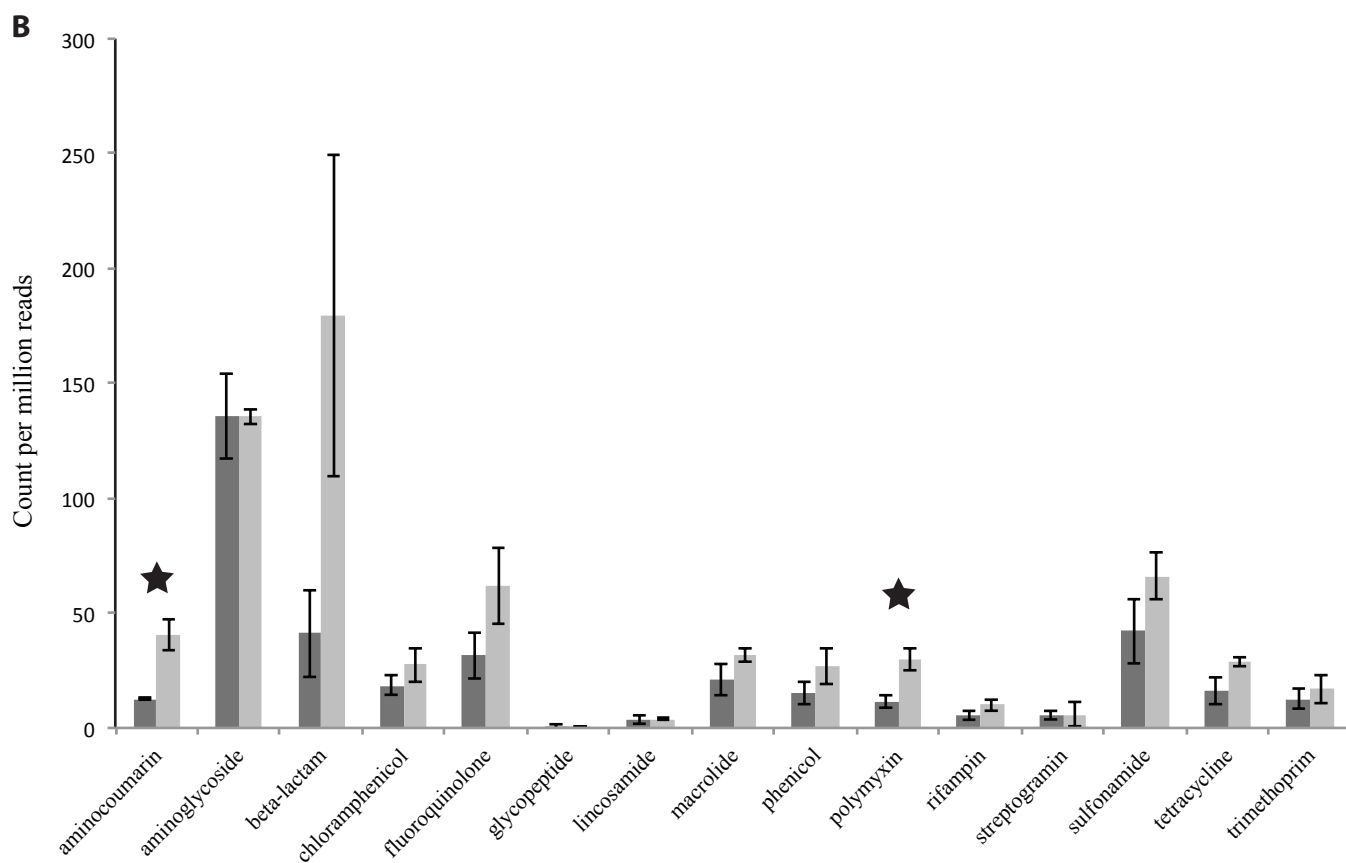
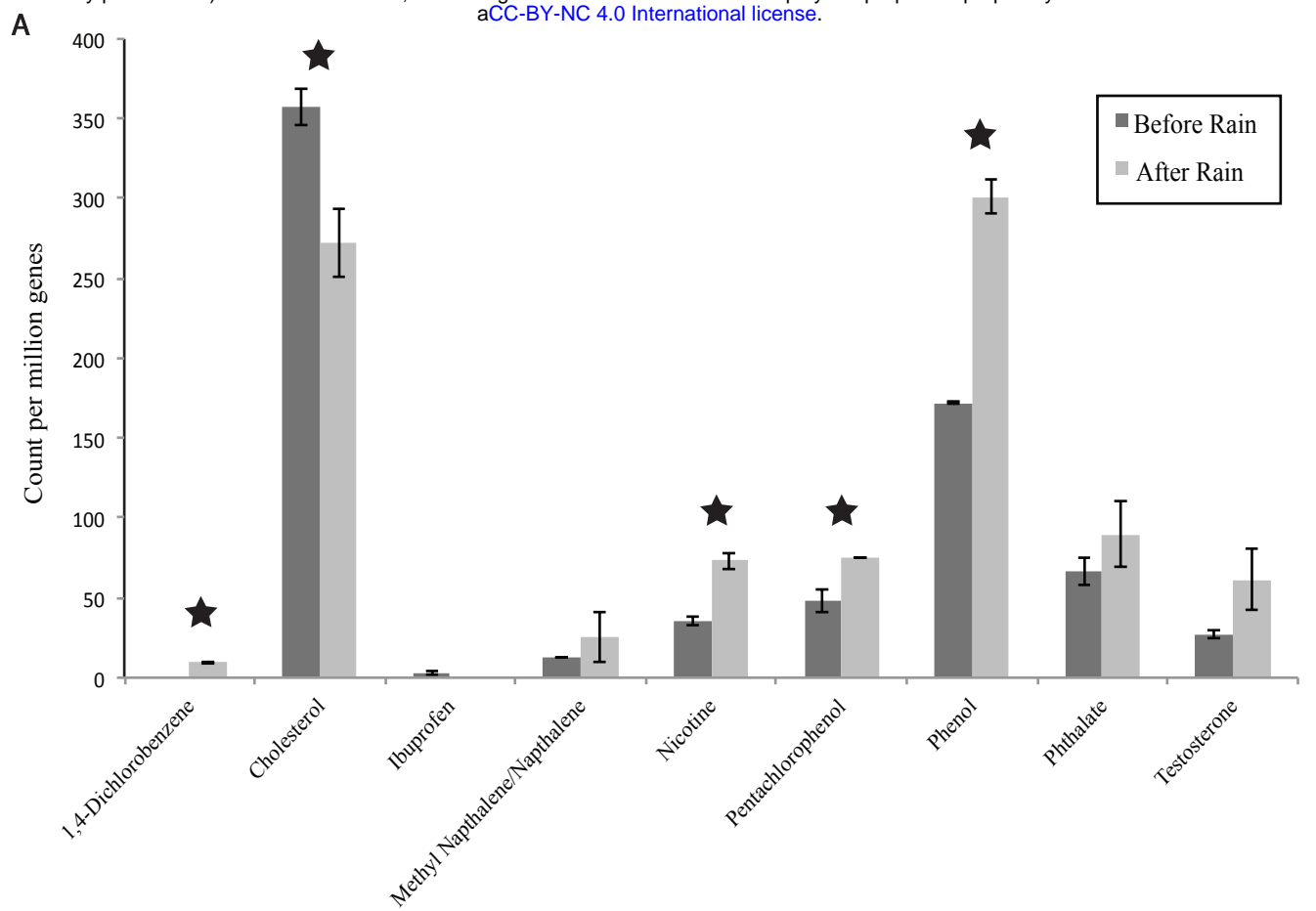


**Figure 4:** Relative abundance of (A) biodegradation genes (BDGs) and (B) antibiotic resistance genes (ARGs) in the before and after rain microbial communities. Relative abundance of BDGs refers to gene count (*in situ* abundance) per million genes per library averaged for each sample for their replicates (n=2) (see Methods section). For ARGs, relative abundance refers to read count per million reads per library averaged for each sample for their replicates. BDGs and ARGs with significant difference in relative abundances between the two time points ( $p < 0.05$ , t-test) are highlighted with stars.